Adsorption and corrosion inhibition behavior of Pterocarpus marsupium stem extract on mild steel in acid medium: Experimental and Statistical approach

Lavanya M
Manipal Academy of Higher Education
Aishwarya S Suvarna
Preethi Kumari P (preethi.prabhu@manipal.edu)
Manipal Academy of Higher Education

Research Article

Keywords: Pterocarpus marsupium, Stem extract, Impedance, Freundlich isotherm, Taguchi

Posted Date: March 29th, 2023

DOI: https://doi.org/10.21203/rs.3.rs-2731030/v1

Abstract

The present work emphasizes the corrosion mitigation behavior of Pterocarpus marsupium stem extract (PMSE) on mild steel (MS) in various concentrations of hydrochloric acid (HCl) solution using an electrochemical technique. The experiments were conducted in three different levels of acid concentrations (0.1, 0.25, and 0.5 M), three levels of inhibitor concentration (0.03, 0.12 and 0.24 g/L), and at three different temperatures (303 to 313 K) and optimized to get maximum inhibition efficiency. The inhibition efficiency increased with an increase in PMSE concentrations in all the acid concentrations and decreased with an increase in temperature. The Tafel polarization technique revealed mixed inhibition behaviour of PMSE with maximum inhibition efficiency (% IE) of 88.9 % at 303 K containing 0.24 g/L of PMSE in 0.1 M HCl solution. The adsorption mechanism of PMSE on the surface of MS is consistent with physisorption by obeying Freundlich's adsorption isotherm. The corrosion inhibition of PMSE predominantly owing to protective film formation on the metal surface and is confirmed by surface morphological and FTIR spectral studies. RSM studies using the Taguchi method revealed the highest inhibition efficiency to be predicted at minimum temperature and acid concentration and at the maximum inhibitor concentration as obtained in the experiments.

1. Introduction

Mild steel (MS) is one of the widely used ferrous alloys, plays a significant role in various industrial and engineering applications due to its tremendous mechanical properties [1]. Although MS has abundant applications, it is much more prone to corrosion because of its thermodynamic instability predominantly in acidic media. As a result of this, the study of the deterioration of MS acidic solution and its protection is considered as an important task from the research point of view [2]. HCl is one of the most frequently used acids for the removal of corrosive products and undesirable oxide film from the surface of metal [3]. Compared to other acids HCl is a more effective and trouble-free acid as it does not hamper the reaction. It finds widespread applications in acidization of oil wells, cleaning of oxide films, and the pickling of metals. Pickling application is one of the greatest benefits of this acid compared to other acids due to the formation of soluble metal chlorides. This greater tendency of solubility of chloride ions leads to minimum polarizing consequence and the rate of reaction remains unaltered. Therefore, the most effective and economic way to control the corrosion of metal is by modifying the corrosive environment. This can be achieved by the addition of inhibitors to the pickling bath. The unique property of these inhibitors is that they act without disturbing the original industrial process [3].

Even though many synthetic compounds exhibit tremendous anticorrosive activity, currently there is limited importance, due to their adverse effects on humans and the environment. Considering the disadvantages of synthetic organic and inorganic inhibitors has inspired the exploration of eco-friendly, biodegradability, and cost-effective alternatives [4]. Research findings have explored extracts from various plant parts and their effectiveness in hindering the corrosion of metals in hostile environments. There are various modern investigations on the corrosion-inhibitive behavior of MS in acidic medium with different stem extracts containing alkaloids, tannin, polyphenolic compounds, carbohydrates, etc. The reported literature includes stem extracts of Sida acuta [5] Ficus racemose [6], Costus Afer [7], Ocimum sanctum [8], Opuntia [9], Corchorus olitorius [10], Olive [11], Cissus populnea [12], Dissotis theifolia [13] showed exceptional inhibiting activity towards MS corrosion in acid medium. These plant extracts emerged as effective corrosion inhibitors due to the existence of complex organic compounds in their configuration. The organic compounds containing heteroatoms such as N, S, and O, the conjugated double and triple bonds, and aromatic rings, serve as the interactive centers between metal surfaces and plant extracts.

The Pterocarpus marsupium belongs to the family Fabaceae and the role of Pterocarpus marsupium as an anti-diabetic has been very well established. It has various medicinal benefits like anti-glycemic, anti-oxidant anti-inflammatory, and also helps in maintaining blood sugar levels [14]. Pterocarpus marsupium contains pterosupin, pterostilbene, liquirtigenin, epicatechin, keno tannic acid, and marsupin as some of the important constituents which are responsible for the attenuation of acid corrosion. These phytochemicals are rich in heteroatoms, electron-donating groups and can have exceptional ability to inhibit acid corrosion. To the best of our knowledge, no literature is available for the stem extract of Pterocarpus marsupium as a corrosion inhibitor for MS in any acidic and alkaline medium.

Mathematical practices can offer valuable qualitative and quantitative proofs, for the enhanced understanding of this corrosion mitigation phenomenon. The design of the experiment (DoE) is a real tool technique for defining new processes and optimization for improved performance. DoE is a statistical and mathematical tool useful to explicate the implication of specific processes and optimize system behavior. It helps in determining the factors with significant aids to the process and also their interaction effects [15]. DoE helps in reducing the number of experiment trials and hence the time and cost of running the experiments [16].

In the current work, a mathematical model was established using RSM and Taguchi, to correlate the association between the input variable [temperature, corrosive media, and inhibitor concentration] with the inhibition response [% IE]. Since the corrosion mitigation process is well explained by combining the experimental and statistical study an effort is made to generate a statistical model to understand the inhibition mechanism along with the influence of the various parameters on it. The Taguchi method is a statistical approach for optimizing design processes using response surface methodology. Optimizing a process is about finding optimum factor levels for peak performance. It gives a design or process which will not only stay within specifications but also be centered at the target with the minimum number of trials. [17, 18] Taguchi method offers a simple and systematic approach to optimize the design for performance, quality as well as cost [19]. Thus, the present investigation is to emphasize the effectiveness of PMSE as a corrosion inhibitor in hydrochloric acid medium with an optimization approach and to carry out corrosion inhibition characteristics using electrochemical measurement.

2. Experimental: Methodology

2.1. Preparation of test coupon and inhibitor solution

MS test coupons with the composition of (% wt.): Carbon (0.432), Silicon (0.187), Manganese (0.496), Phosphorous (0.060), Sulphur (0.011), Chromium (0.047), Nickel (0.06), Molybdenum (0.019), Aluminium (0.039), Copper (0.0015) and Iron (98.51) was used in the present study. Cylindrical test coupons of MS metal having 1cm^2 exposed surface area were mounted with cold setting resin. They were abraded with emery papers ranging from 200 to 1500 grades to get a highly smooth surface and further polished on a disk polisher with alumina abrasive. Finally, the test coupons are cleaned with distilled water, and it is dried before immersing into the corrosive media. The standard solution of HCl was prepared using 37% AR grade HCl and double-distilled water.

Fresh Pterocarpus marsupium stem powder was procured from Chemiloids Hyderabad. The stock solution of aqueous extract PMSE is prepared by dissolving the known weight sample in 1 litre of acid medium. The required concentration is prepared as and when required by diluting the stock solution. The experiments were conducted at the temperature range of 303–323 K, in a thermostat calibrated up to ±0.5 °C under unstirred conditions.

2.2. Electrochemical measurements

Electrochemical tests such as Tafel polarization (TP) was carried out as reported in the literature [20] in a conventional Pyrex glass cell using an electrochemical work station (CH Instrument USA Model 604D series with beta software). The metal under corrosion is used as a working electrode, platinum as a counter, and calomel as the reference electrode. Freshly polished MS coupons were immersed in a conductive medium of HCl with and without PMSE at various temperatures for 30 minutes and allowed to obtain open circuit potential (OCP). TP parameters such as corrosion potential (E_{corr}) and corrosion current density (i_{corr}) were recorded from the Tafel plots are used to estimate corrosion rate (CR) and percentage inhibition efficiency (% IE).

2.3. Fourier Transform Infra-red (FTIR) spectral analyses

Shimadzu IR spirit spectrophotometer was used to record the FTIR spectrum of PMSE solid and the scraped-out product of the adsorbed protective layer formed on the MS surface exposed to 0.24 g/L PMSE in 0.5 M HCl acid solution.

2.4. Surface topography studies

Freshly polished MS metal coupons were introduced in 0.5 M HCl solution in the absence and presence of PMSE to carry out surface morphological studies using JEOL JSM–6380L scanning electron microscope (SEM) and 1B342 Innova atomic force microscope (AFM).

2.5. Response Surface Analysis

HCl concentration, PMSE concentration and temperature were taken as input parameters to optimize the inhibition efficiency using the Taguchi method. A set of experiments were generated at 3 levels of the input parameters using the Design-Expert® software.

3. Results And Discussion

3.1. Electrochemical Studies

3.1.1. Open Circuit Potential

It is significant to provide the steady-state potential of the metal surface before the electrochemical tests as it helps to understand the behavior of metals in electrochemical reactions in a given medium. The variation of open circuit potential (OCP) with time is represented in Fig.1 and it is observed that MS acquired steady-state OCP in 1800 sec. The OCP value at different concentrations of PMSE is found to increase from -0.54 V and reach a steady state in the range of -0.51 V in 0.5 M HCl. The increase in OCP value attributes to the rupture of the pre-immersion air-formed oxide layer while constant potential value contributes to the further thickening of the oxide layer [21,22]. The small positive variation in potential overtime for the inhibited solution compared to the blank attributed to the formation of corrosion products and/or adsorption of inhibitor molecules on the metal surface that offered partial protection of the material [23, 24].

3.1.2. Tafel polarization (TP) Studies

The influence of different concentrations of PMSE on MS corrosion was monitored by the TP method and the resulting TP plots for the metal dissolution in various concentrations of HCl solution are depicted in Fig.2 (a). The i_{corr} and E_{corr} are obtained by the linear extrapolation of cathodic and anodic curves and the point of intersection corresponding to the x-axis and y-axis respectively. It is observed from the Tafel plots that the addition of PMSE to the acid environment leads to the shift in cathodic and anodic current curves toward the lower current densities thereby causing a substantial reduction in the CR [26].

The *CR*, the degree of surface coverage (Θ), and the % *IE* were obtained from Eqs. (1), (2) and (3) respectively [27].

$$CR(mmy^{-1}) = \frac{3270 \times EW \times i_{corr}}{d} \qquad (1)$$

Where 3270 is constant that describes the unit for the corrosion rate, i_{corr}= corrosion current density in μA/cm^2, *d*= density of corroding material in g/cm^3, *EW* = equivalent weight of corroding metal (atomic weight/ number of electrons transferred per atom.

$$\theta = \frac{i_{corr} - i_{corr(inh)}}{i_{corr}} \qquad (2)$$

where, θ is the surface coverage, i_{corr} and $i_{corr(inhi)}$ are the corrosion current densities with and without PMSE respectively [28]. The results of the PDP technique are recorded in Table 1.

$$\%IE = \theta \times 100 \qquad (3)$$

It is evident from the literature if the difference in E_{corr} is greater or lesser than ±85 mV compared to the E_{corr} of the uninhibited solution then the inhibitor can be regarded as an anodic or cathodic type [29]. Since in the present study, the maximum shift in corrosion potential is less than 85 mV suggesting mixed behavior of PMSE. The increase in the % IE with an increase in PMSE concentration is attributed to the increase in the surface coverage of MS surface by the adsorbed PMSE molecules in all the concentrations of HCl. Further, the percentage inhibition efficiency decreased with an increase in acid concentration. This may be due to the increase in the aggressiveness of the corrosive medium causing more dissolution of metal [30].

3.1.3. Effect of Temperature

Temperature is another factor having a greater influence on the conductivity of the corrosive medium. The increase in the conductivity of solution leads to the desorption of adsorbed PMSE molecules from the metal surface which will be the cause of decreasing trend in the % IE with rising in temperature as depicted in Fig. 2(b) [31]. This also signifies the physisorption of PMSE onto the metal surface.

The corrosion rate values obtained for the MS sample immersed in different concentrations of HCl containing various concentrations of PMSE at various temperatures facilitate the measurements of activation and thermodynamic parameters. The energy of activation (E_a) is calculated using Arrhenius Eq. (4) [32].

$$\ln(CR) = B - \frac{E_a}{RT} \quad (4)$$

where B is the Arrhenius constant, and R is the universal gas constant. The plot of ln (CR) versus 1/T (Fig. 3(a) gives a straight line with slope = - Ea/R, from which, the activation energy values for the corrosion process were calculated. The change in enthalpy (ΔH#) and change in entropy (ΔS#) of activation for the metal dissolution process in the absence and presence of PMSE is determined using the transition state Eq. (5) [33] and the resultant activation parameters are given in Table 2.

$$CR = \frac{RT}{Nh}\exp\left(\frac{\Delta S^{\neq}}{RT}\right)\exp\left(\frac{-\Delta H^{\neq}}{RT}\right) \quad (5)$$

where h is Plank's constant and N is Avogadro's number. A plot of ln (CR/T) versus 1/T gave a straight line (Fig.3 (b)) withslope = $\Delta H^{\#}$/R and intercept = ln (R/Nh) + ($\Delta S^{\#}/R$).

From Table 2 it is observed that E_a values rise after successive addition of the PMSE which attributes to physisorption. Further, the E_a value in the absence and presence of the PMSE is more than 20 kJmol^{-1} which ascribes that the entire process is regulated by the surface reaction. E_a values are more pronounced with inhibitor concentration which describes the reduction in the dissolution of metal in the acid medium after the addition of PMSE. This indicates the increase in the energy barrier of the corrosion process due to the adsorption of active organic molecules at the MS surface [34]. The large negative values of entropy of activation ($\Delta S^{\#}$) in inhibited and uninhibited solution infer that the activated complex in the rate-determining step represents an association rather than dissociation, leading to a decrease in the randomness ongoing from the reactants to the activated complex [35].

3.1.4. Adsorption isotherm

Adsorption isotherms refer to the relationship between the PMSE concentrations in the liquid phase and the adsorption amount of PMSE on the solid phase at a certain temperature range. The adsorption behaviour of PMSE at mild steel/solution interface can be interpreted by choosing a suitable isotherm, which ascribes the deviation of the amount of adsorbed material per unit area at the mild-steel surface with its bulk concentration [36]. The degree of surface coverage (θ) values acquired from TP studies are used fitted to various adsorption isotherms such as Temkin, Freundlich, Frumkin, Langmuir. The best correlation was acquired for Freundlich adsorption isotherm and it is given by the Eq. (6).

$\log q = \log K + 1/n \log C$ (6)

C is the concentration of inhibitor and K_{ads} is the equilibrium constant of adsorption reaction [37].

The graph of log θ versus log C (Fig. 4) shows a straight line and values of K_{ads} are calculated from the intercept. The K_{ads} values are then used to calculate the standard free energy of adsorption ($\Delta G°_{ads}$) by the relation (7) [37].

K_{ads} = (1/55.5) exp (-$\Delta G°_{ads}$ / RT) (7)

Where R is the universal gas constant, T is the absolute temperature, and 55.5 is the concentration of water in solution in mol dm^{-3}. The enthalpy and entropy of adsorption values are calculated from thermodynamic Eq. (8). The thermodynamic parameters provide valuable evidence about the corrosion inhibition process and are tabulated in Table.3.

$$\Delta G^{o}_{ads} = \Delta H^{o}_{ads} - T\Delta S^{o}_{ads} \quad (8)$$

From Table 3 it is observed that with an increase in temperature K_{ads} values decrease. The adsorption coefficient attributes to the rate of adsorption of inhibitor onto the metal surface. In the present study, it was found that greater values of K_{ads} at low temperatures, ascribes to stronger adsorption of inhibitor molecules onto the surface of metal [38]. With an increase in temperature, there may be a decrease in the adsorption of inhibitor molecules suggesting the physical adsorption of PMSE molecules on the metal surface.

Since the obtained ΔG°_{ads} values are less negative than -20 kJ/mol signify that the adsorption of PMSE on the metal surface is based on physical adsorption [39, 40]. If the values of ΔH°_{ads} are more positive (endothermic process) attributes to chemical adsorption whereas ΔH°_{ads} is more negative (exothermic process) attributes to chemisorption or physisorption or a mixture of both [41, 42]. In the present study, the negative values of ΔH°_{ads} specify the physical adsorption of the molecule. The ΔS°_{ads} value is negative indicates, random displacement of the PMSE molecules in the bulk of the solution before the adsorption on the surface of the metal but as the adsorption proceeds the inhibitor molecules were evenly adsorbed on the surface of the metal, escorted to reduction in entropy [43].

3.2. Mechanism of corrosion

The factors that influence the adsorption of inhibitor molecule on the metal surface depends on the chemical structure, charge on the inhibitor, and behavior of the acidic media. Generally, the adsorbed inhibitor molecules block the active sites on the metal leading to the formation of a barrier layer at the metal solution interface. PMSE contains a large number of heterocyclic rings, electron-donating groups, flavonoids, tannins, etc., which get adsorb on the surface of the metal, forming a protective film and hence protecting the metal from dissolution. Generally, inhibitor molecules may adsorb on the surface of the metal, either by physisorption or by chemisorption, or by mixed adsorption. Physical adsorption takes place by the electrostatic interaction between the protonated inhibitor and chloride ions that are previously adsorbed on the surface of the metal. Chemisorption focuses on donor-acceptor interaction between the π-electrons of aromatic ring & metal surface containing empty d-orbitals or by the interaction between hetero atom having unshared electron pair and & metal surface containing vacant d orbitals. Thermodynamic parameters revealed the adsorption of PMSE on MS via physical mode. Schematic representation for a physical mode of adsorption is depicted in Fig.5.

MS specimen immersed in the acidic environment gets positively charged due to its initial dissolution which favors the adsorption of negatively charged chloride ions towards the vicinity of the metal surface. This results in the formation of Helmholtz electrical double layer at the metal solution interface which then promotes the adsorption of protonated PMSE molecules onto the metal surface by electrostatic interaction [44].

3.3. FTIR Characterization of PMSE

The FTIR spectrum of stem extract of PM and the corroded product after its inhibition is shown in Fig.6. The peak corresponding carbonyl group at 1600 cm-1 is slightly shifted to 1650 cm-1, and the peak with respect to –OCH3 is shifted from 1200 to 1300 cm-1 indicating the adsorption active constituents of extract molecules onto the metal surface. The reduction in the intensity of the peak at around 2900 cm-1 indicates the decrease in the aromaticity of the molecules due to the adsorption of π electrons of the benzene ring present in the extracted molecule. The broad peak at 3300 cm-1 is due to the presence of –OH group. The lone pair of electrons of the oxygen atom donated to the metal making the bond order of C-O increase slightly which is reflected in the peak around 3200cm-1suggesting the bond formation between the adsorbed molecule and metal surface.

3.4. Surface morphological study

Surface characterization is done using a Scanning electron microscope (SEM) and atomic force microscope (AFM) to investigate the changes that occurred on the surface of MS specimen in the absence and presence of PMSE. The SEM image of (a) corroded MS (b) MS dipped in 0.1 M HCl containing PMSE is shown in Fig.7. Fig. 7 (a) exhibits a rough surface with more number pits and is severely corroded by the attack of acid. However, in presence of PMSE (Fig. 7b) smooth surface was obtained without any pits which confirm the adsorption of PMSE onto the surface of the metal.

The three-dimensional AFM images of the MS treated with acid and acid-containing PMSE are depicted in Fig. 8 (a) and (b) respectively. Table 4, comprises the average surface roughness (Ra) and root mean square (RMS) roughness (Rq). From Table 4 it is observed that average surface roughness is greater for uninhibited specimens when compared to the inhibited specimen. The lesser values of Rq and Ra for the inhibited sample are attributed to the formation of the protective layer of PMSE onto the metal surface and prevent further corrosion [45].

4. Response Surface Methodology

The inhibition efficiency of PMSE adsorbed on the surface of MS towards corrosion caused by HCl was analysed by the Taguchi method. Three input parameters were taken into consideration, namely A- HCl concentration (HCl conc), B- Inhibitor concentration (Inh conc), and C- Temperature (Temp). Table 5 shows the considered parameters and the three selected levels for each of them.

The analysis revealed a significant model with an F-value of 18.01 with only 0.29 % of such a large F-value occurring due to noise. B was found to be the only significant parameter with a p-value of 0.0029. Further fit statistics obtained for the model are: R^2, adjusted R^2, and predicted R^2 of 0.8572, 0.8096, and 0.6787 respectively. The adequate precision that measures the signal to noise ratio was to have a value of 8.465. Since this ratio is greater than 4, the model indicates adequate signal and can be used to navigate the design space [46]. Since the predicted R^2 is in reasonable agreement with the adjusted R^2 having a difference less than 0.2, it can be said that the model can explain 80.96 % and 67.87 % of the values obtained for the experimental and predicted values for oil removal respectively.

The final equation in terms of the coded factors can be shown in Eq. (9). This equation can be used to make predictions about the response for given levels of the factor B. In general, the coded equation is useful for identifying the relative impact of the factors by comparing the factor coefficient.

$$IE = 54.32 - 19.97\,B[1] - 1.74\,B[2] \quad (9)$$

We see from Fig. 9 that the predicted vs actual values of IE are in an agreeable form. The same can be observed from the plot of Cook's distance showing no outliers in the model obtained from the experimental values.

3.4.1. Interactive Effect

Response surface plots for IE were used to interpret the interaction effect of the variables and are shown in Fig. 10. The plots were utilized to explain the combined effects of the process parameters on the inhibition efficiency. The surface plots were generated from the model by varying any two variables within the range of the experimental data while keeping the other independent factors at their midpoint.

The nature of the plot can indicate the amount of effect the parameters have on the oil removal. The slightly straight, unchanged bard in Fig. 10 (b) indicate the very little effect of temperature and HCl concentration on the inhibition efficiency. Whereas Fig. 10 (a) and (c) shows a significant combined effect of the axes parameters on IE. Fig. 10 (a) is the surface plot observing the interaction effect between inhibitor concentration and HCl concentration at a temperature of 313 K. The increase in the inhibitor concentration and fall in HCl concentration results in the increase in inhibition efficiency. A maximum IE of 82.6 % was observed at inhibitor concentration of 0.24 M and HCl concentration of 0.1 M. Fig. 10 (b) observes the interaction effect between temperature and HCl concentration at a constant inhibitor concentration of 0.12 M. The inhibition efficiency is observed to increase with a decrease in the temperature and HCl concentration. A maximum IE of 68.7 % was predicted at temperature 303 K and HCl concentration of 0.1 M.

Fig. 10 (c) observes the interaction effect between inhibitor concentration and temperature at a constant HCl concentration of 0.25 M. The rise in inhibitor concentration coupled with a reduced temperature results in an increase in the inhibition efficiency. A maximum oil removal of 85.33 % was predicted at temperature 313 K and inhibitor concentration of 0.24 M.

The above effects can also be observed in the graphs shown in Fig. 11. The plots also further show that the inhibitor concentration has a significant effect over the inhibition efficiency, and that HCl concentration and inhibitor concentration do not effect it as much. HCl provides the acidic medium for corrosion to take place. At lower HCl concentrations, the acidic content of the medium is not enough to break through the inhibitor barrier adsorbed over the mild steel. Hence the inhibition efficiency is higher. With the increase in HCl concentration, the acidic medium gets stronger and breaks through the barrier lowering the inhibition efficiency [47].

With increasing concentrations of the inhibitor, PMSE got better adsorbed onto the surface of mild steel, decreasing the interaction with HCl and forming a barrier to prevent further corrosion [48]. With larger concentrations, the inhibitor layers over the surface of mild steel significantly affect corrosion [49, 50].

When the temperature of the medium increases, surface coverage reduction causes the desorption of PMSE inhibitor from the mild steel surface and the mild steel surface is exposed to the acidic medium. This can be attributed to the decrease in the strength of the adsorption process at higher temperatures as a result of the physical adsorption of the inhibitor on the mild steel, thus resulting in decreased inhibition efficiency with increasing temperature [51-53].

3.4.2. Optimization of IE

The optimized parameters to get the maximum IE based on RSM were obtained from the model generated by the Design Expert software by keeping HCl concentration and temperature fixed at 0.1 M and 303 K respectively. The maximum IE was predicted to be 76.0267 % at an inhibitor concentration of 0.24 M with a desirability of 0.76. This, when compared to the observed inhibition efficiency of 88.9 % gave an error of 14.48 %.

4. Conclusions

The aqueous extract of *Pterocarpus marsupium* (PMSE) stem has not been explored as a corrosion inhibitor for MS in an acidic environment. The following conclusions can be drawn from the present work:

- The PMSE displayed inhibition maximum efficiency of 88.9 % in 0.1 M HCl solution, presenting a mixed-type inhibition
- The adsorption of PMSE agreed with Freundlich's isotherm model and the electrostatic interaction between the inhibitor molecules and the metal surface accounted for the physical adsorption of PMSE
- The resulting activation and thermodynamic parameters support the physical adsorption of PMSE molecules
- SEM and AFM analysis confirmed the remarkable adsorption ability of the PMSE molecules on the MS surface, thereby blocking the reactive sites
- FTIR spectrum of scraped PMSE product from the metal surface confirmed the adsorption of PMSE molecules on the MS surface
- RSM analysis confirms the experimental results of the inhibition efficiency predicting the optimum temperature and acid concentrations to be low and the inhibitor concentration

Declarations

Acknowledgments

Authors acknowledge the laboratory facility extended by the Department of Chemistry, MIT, MAHE.

Competing interests

On behalf of all the authors, the corresponding author claims no competing interest.

Authors' contributions

Lavanya M carried out the statistical study, Aishwarya S Suvarna has done the corrosion study using electrochemical measurement and Preethi Kumari P has done the analysis of experimental results and manuscript preparation.

Funding

We have not received any funding for the above research work carried out.

Availability of data and materials

Not applicable

References

1. Prabakaran M, Kim SH, Hemapriya V, Gopiraman M, Kim IS, Chung IM (2016) Rhus verniciflua as a green corrosion inhibitor for mild steel in 1 M H_2SO_4, R. Soc. Chem. 6:57144- 57153. https://doi.org/10.1039/C6RA09637A.
2. Amin MA, Abd El-Sherbini SS, El-Sherbini EEE, Bayoumi RS (2007) The inhibition of low carbon steel corrosion in hydrochloric acid solutions by succinic acid Part I. Weight loss, polarization, EIS, PZC, EDX and SEM studies. Electrochem 52:3588–3600. https://doi.org/10.1016/j.electacta.2006.10.0193.
3. Krishnegowda PM, Venkatesha VT, Krishnedowda PKM, Shivayogiraju SB (2013) Acalypha torta leaf extract as green corrosion inhibitor for mild steel in hydrochloric acid solution. J Ind Eng Chem 52:722–728. https://doi.org/10.1021/ie3018862.
4. De lima KCS, Paivaa VM, Ripper B (2020) Glycine max meal extracts as corrosion inhibitor for mild steel in sulphuric acid solution. J Mater Res Technol 9:12756–12772. https://doi.org/10.1016/j.jmrt.2020.09.019.
5. Umoren SA, Eduok UM, Solomon MM, Udoh AP (2011) Corrosion inhibition by leaves and stem extracts of Sida acuta for mild steel in 1 M H2SO4 solutions investigated by chemical and spectroscopic techniques. Arab J Chem 9:209-224. https://doi.org/10.1016/j.arabjc.2011.03.008.
6. Bagga MK, Gadi R, Yadav OS, Kumar R, Chopra R, Singh G (2016) Investigation of phytochemical components and corrosion inhibition property of Ficus racemosa stem extract on mild steel in H2SO4 medium. Biochem Pharmacol 4:4699-4707. https://doi.org/10.1016/j.jece.2016.10.022.
7. Uwah IE, Ugi BU, Ikeuba AI, Etuk KE (2013) Evaluation of the inhibitive action of eco- friendly benign costus afer stem extract on the corrosion of mild steel in 5 M HCl solution. ISDS 2:1970–1981.
8. Kumpawat N, Chaturvedi A, Upadhyay RK (2010) A comparative study of corrosion Inhibition efficiency of stem and leaves extract of ocimum sanctum (holy basil) for mild steel in HCl solution. Prot Met Phys Chem 46:267-270. https://doi.org/10.1134/S2070205110020152.
9. Honarmand E, Mostaanzadeh H, Hassan M, Motaghedifardb Hadia M, Khayadkashani M (2017) Inhibition effect of opuntia stem extract on corrosion of mild steel: a quantum computational assisted electrochemical study to determine the most effective components in inhibition. Prot Met Phys Chem 53:560–572. https://doi.org/10.1134/S207020511703008X.
10. Oyewole O, Oshin TA, Atotuoma BO (2021) Corchorus olitorius stem as corrosion inhibitor on mild steel in sulphuric acid. Heliyon 7:2405-8440. https://doi.org/10.1016/j.heliyon.2021.e06840.
11. Bouknana D, Hammouti B, Serghini H, Jodeh S, Bouyanzer A, Aouniti A, Warad I (2015) Aqueous extracts of olive roots, stems, and leaves as eco-friendly corrosion inhibitor for steel in 1 M HCl medium. Int J Ind Chem 6:233–245. https://doi.org/10.1007/s40090-015-0042-z.
12. Chahul HF, Orhemba DT, Gbadamosi TA (2019) Influence of cissus populnea stem extract on kinetics and thermodynamics of MS corrosion in acidic medium. OUAC 30:14–20. https://doi.org/10.2478/auoc-2019-0003.
13. Iroha NB, Jane MN (2020) Stem extract of discotic the folia (Melastomataceae) as a green corrosion inhibitor for N80 steel in 1 M HCl solution. ISOR-JAC 13:30-38.
14. Deepti K, Vijender S, Ali M (2016) Phytochemical and pharmacological profile of Pterocarpus marsupium: A review, J Pharm Innov 5(4): 31-39.

15. Lavanya M, Rao P, Murthy VR, Selvaraj S (2020) Parametric study of aluminium alloy fouling in marine environment using RSM technique. Tribol-Mater Surf Interface 14:110–118. https://doi.org/10.1080/17515831.2019.1690406.
16. Akbarzadeh E, Ibrahim MNM, Rahim AA (2012) Monomers of lignin as corrosion inhibitors for mild steel: study of their behavior by factorial experimental design. Corros Eng Sci Technol 47:302–311. https://doi.org/10.1179/1743278212Y.0000000013.
17. Siroos S, Saeed S, Shahab SB, Amir Abbas KF, Milad G, Amir M (2021) Application of Taguchi method and response surface methodology into the removal of malachite green and auramine-O by NaX nanozeolites, Sci Rep. 11:16054. https://doi.org/10.1038/s41598-021-95649-5.
18. Tong Li, Su CT, Wang CH (1997) The optimization of multi-response problems in the Taguchi method. Int J Qual Reliab Manage. 14:367–380. https://doi.org/10.1108/02656719710170639 .
19. Ali Fathima A, Sabirneeza S, Rajalakshmi R (2013) Water soluble conducting polymer composite of polyvinyl alcohol and leucine: an effective acid corrosion inhibitor for mild steel. Mater Corros 64:74–82. https://doi.org/10.1002/maco.201106096.
20. Kumari P, Shetty P, Rao S (2017) Electrochemical measurements for the corrosion inhibition of mild steel in 1 M hydrochloric acid by using an aromatic hydrazide derivative. Arabian J Chem 10:653–663. https://doi.org/10.1016/j.arabjc.2014.09.005.
21. Abd El Aal EE, Abd El Haleem SM (2008) Kinetics of oxide film growth and destruction on iron surface in carbonate solutions. Int J Corros 43:219-224. https://doi.org/10.1179/174327807X214905.
22. Sigircik G, Tuken T, Erbil M (2015) Assessment of the inhibition efficiency of 3,4-diaminobenzonitrile against the corrosion of steel. Case Stud Fire Saf 102:437-445. https://doi.org/10.1016/j.corsci.2015.10.036.
23. Zhao Y, Pan T, Yu X, Chen D (2019) Corrosion inhibition efficiency of triethanolammonium dodecylbenzene sulfonate on Q235 carbon steel in simulated concrete pore solution. Corros Sci 158:1-12. https://doi.org/10.1016/j.corsci.2019.108097.
24. Saxena A, Prasd D, Haldhar R, Singh G, Kumar A (2017) Use of Sida cordifolia Extract as Green Inhibitor for mild steel in 0.5 M H2SO4. J Environ Chem Eng 6:694-700. https://doi.org/10.1016/j.jece.2017.12.064.
25. Kumari P, Shetty P, Rao S (2014) Corrosion inhibition effect of 4-Hydroxy-N' -[(E)-(1H-indole-2-ylmethylidene)] Benzohydrazide on mild steel in hydrochloric acid solution. Int J Corros 2014:1-11. https://doi.org/10.1155/2014/256424.
26. Shanbhag AV, Venkatesha TV, Prabhu RA, Kalkhambkar RG, Kulkarni GM (2007) Corrosion inhibition of mild steel in acidic medium using hydrazide derivatives. J Appl Electrochem 38:279–287. https://doi.org/10.1007/s10800-007-9436-8.
27. Kagatikar S, Sunil D, Kumari P (2020) Investigation of anticorrosive property of carbazolecarbaldehyde azine on mild steel using electrochemical, morphological and theoretical studies. J Bio-Tribo-Corros 6:1-17. https://doi.org/10.1007/s40735-020-00433-z.
28. Saxena A, Prasad D, Haldhar R (2018) Use of Asparagus racemosus extract as green corrosion inhibitor for mild steel in 0.5 M H2SO4. J Mater Sci 53:8523–8535. https://doi.org/10.1007/s10853-018-2123-9.
29. Li W, He Q, Zhang S, Pei C, Hou B (2007) Some new triazole derivatives as inhibitors for mild steel corrosion in acidic medium. J Appl Electrochem 38:289-295. https://doi.org/10.1007/s10800-007-9437-7.
30. Schmid GM, Huang HJ (1980) Spectro-electrochemical studies of the inhibition effect of 4, 7-diphenyl -1, 10-phenanthroline on the corrosion of 304 stainless steel. Corros Sci 20:1041–1057.

https://doi.org/10.1016/0010-938X(80)90083-9.

31. Ahamad I, Quraishi MA (2010) Mebendazole: new and efficient corrosion inhibitor for mild steel in acid medium. Corros Sci 52:651–656. https://doi.org/10.1016/j.corsci.2009.10.012.
32. Bhat JI, Alva VDP (2011) A study of aluminium corrosion inhibition in acid medium by an antiemitic drug. Trans Indian Inst Met 64:377–384. https://doi.org/10.1007/s12666-011-0102-9.
33. Prabakaran M, Kim S, Mugila N (2017) Aster koraiensis as nontoxic corrosion inhibitor for mild steel in sulfuric acid. J Ind Eng Chem 52:235-242. https://doi.org/10.1016/j.jiec.2017.03.052.
34. Elayyachy M, El Idrissi A, Hammouti B (2006) New thio-compounds as corrosion inhibitor for steel in 1 M HCl. Corros Sci 48:2470–2479. https://doi.org/10.1016/j.corsci.2005.09.016.
35. Olivares O, Likhanova NV, Gomez B, Navarrete J, Llanos-Serrano, ME, Aece E, Hallen JM (2006) Electrochemical and XPS studies of decylamides of α-amino acids adsorption on carbon steel in acidic environment. Appl Surf Sci 252:2894–2909. https://doi.org/10.1016/j.apsusc.2005.04.040.
36. Tebbji K, Faska N, Tounsi A, Ouddha H, Benkaddour M, Hammouti B (2007) The effect of some lactones as inhibitors for the corrosion of mild steel in 1 M hydrochloric acid. Mater Chem Phys 106:260–267. https://doi.org/10.1016/j.matchemphys.2007.05.046.
37. Elachouri M Hajji MS, Salem M, Kertit S, Aride J, Coudert R, Essasssi E (1996) Some nonionic surfactants as inhibitors of the corrosion of iron in acid chloride solutions. Corros. Sci. 52:103-108. https://doi.org/10.5006/1.3292100.
38. Quraishi MA, Sharma HK (2003) 4-Amino-3-butyl-5-mercapto-1,2,4-triazole: a new corrosion inhibitor for mild steel in sulphuric acid. Mater Chem Phys 78:18–21. https://doi.org/10.1016/S0254-0584(02)00313-9.
39. Gomma GK, Wahdan MH (1995) Schiff bases as corrosion inhibitors for aluminium acid solution in hydrochloric. Mater Chem Phys 39:209-213. https://doi.org/10.1016/0254-0584(94)01436-K.
40. Durnie W, Marco R, Jefferson A, Kinsella B (1999) Development of a structure-activity relationship for oil field corrosion inhibitors. J Electrochem Soc 146:1751–1756. https://doi.org/10.1149/1.1391837.
41. Tang L, Mu G, Liu G (2003) The effect of neutral red on the corrosion inhibition of cold rolled steel in 1.0 M hydrochloric acid. Corros Sci 45:2251–2262. https://doi.org/10.1016/S0010-938X(03)00046-5.
42. Dahiya S, Kumar P, Lata S, Kumar R, Dahiya N, Ahlawat S (2017) An exhaustive study of a coupling reagent (1-(3-dimethylaminopropyl) 3-ethylcarbodiimide hydrochloride) as corrosion inhibitor for steel. Indian J Chem Technol 24:327–335. https://www.researchgate.net/publication/317175437.
43. Verma DK, Khan F, Bahadur I, Salman M, Quraishi MA, Verma C, Ebenso E (2018) Inhibition performance of Glycine max, Cuscuta reflexa and Spirogyra extracts for mild steel dissolution in acidic medium: Density functional theory and experimental studies. Results Phys 18:665-674. https://doi.org/10.1016/j.rinp.2018.06.003.
44. Ahamad I, Khan S, Ansari KR, Quraishi MA (2011) Primaquine: A pharmaceutically active compound as corrosion inhibitor for mild steel in hydrochloric acid solution. J chem Pharm 3:703-717. https://www.researchgate.net/publication/287529487.
45. Stat-Ease » v11 » Adequate Precision (accessed Feb. 06, 2023) https://www.statease.com/docs/v11/navigation/adequate-precision/
46. Parameswari K, Rekha S, Chitra S, Kayalvizhy E (2010) Study on the Inhibition of Mild Steel Corrosion by Benzoisoxazole and Benzopyrazole Derivatives in H_2SO_4 Medium. Port Electrochim Acta 28:189-201. http://dx.doi.org/10.4152/pea.201003189.

47. Ahmed A. Al-Amiery, Abu Bakar Mohamad, Abdul Amir H. Kadhum, Lina M. Shaker, Wan Nor Roslam Wan Isahak, Mohd S. Takriff (2022) Experimental and theoretical study on the corrosion inhibition of mild steel by nonanedioic acid derivative in hydrochloric acid solution. Sci Rep 12:4705. https://doi.org/10.1038/s41598-022-08146-8.
48. Rathika G, Swetha A (2015) Study of corrosion inhibition properties of novel semicarbazones on mild steel in acidic solutions. J Chil Chem Soc 60:2786- 2798. http://dx.doi.org/10.4067/S0717-97072015000100004.
49. Laamari MR, Benzakour J, Berrekhis F, Derja A, Villemin D (2016) Adsorption and corrosion inhibition of carbon steel in hydrochloric acid medium by hexamethylenediamine tetra(methylene phosphonic acid). Arabian J Chem. 9:245-251. http://dx.doi.org/10.1016/j.arabjc.2011.03.018.
50. Ebenso, Eno, Obot, Ime (2010) Inhibitive Properties, Thermodynamic Characterization and Quantum Chemical Studies of Secnidazole on Mild Steel Corrosion in Acidic Medium. Int. J. Electrochem. Sci. 5:2012-2035. https://www.researchgate.net/publication/261725478.
51. Maayta AK, Al-Rawashdeh NAF (2004) Inhibition of acidic corrosion of pure aluminum by some organic compounds. Corros Sci 46:1129-1140. https://doi.org/10.1016/j.corsci.2003.09.009.
52. Abboud Y, Abourriche A, Saffaj T, Berrada M, Charrouf M, Bennamara A, Hannache H (2009) A novel azo dye, 8-quinolinol-5-azoantipyrine as corrosion inhibitor for mild steel in acidic media. Desalination 237:175-189. https://doi.org/10.1016/j.desal.2007.12.031.

Tables

Table 1 Result of Tafel polarization for the corrosion of MS in various concentrations of hydrochloric acid in the absence and presence of PMSE at different temperatures

Temp (K)	Conc. Inh.	0.1 M			0.25 M			0.5 M		
	(M)	i_{corr}	CR	%IE	i_{corr}	CR	%IE	i_{corr}	CR	%IE
303K	0	4.127	1120	-	5.321	1237	-	6.129	1356	-
	0.03	2.414	655.2	41.5	3.395	789.2	36.2	4.133	945.1	31.5
	0.12	1.292	350.6	68.7	2.304	536.5	56.7	3.158	721.1	47.5
	0.24	0.458	124.3	88.9	0.782	182.1	85.3	1.260	288.1	79.1
313K	0	6.427	1519	-	7.142	1629	-	7.950	1818	-
	0.03	4.133	976.7	35.7	4.757	1084.9	33.4	5.582	1276	29.7
	0.12	2.481	586.3	61.4	3.350	764.0	53.1	4.581	1048	42.3
	0.24	1.118	264.3	82.6	1.721	392.6	75.9	2.831	647.4	64.3
323K	0	5.787	2129	-	7.645	2300	-	10.92	2497	-
	0.03	3.866	1422.2	33.2	5.283	1589.5	30.8	7.858	1797	28.1
	0.12	2.598	955.9	55.1	3.922	1179.9	48.7	6.559	1500	40.0
	0.24	1.250	459.9	78.4	2.660	800.4	65.2	5.103	1167	53.2

Table 2 Activation parameter for the corrosion of MS in different concentrations of hydrochloric acid containing different concentrations of PMSE

	0.1 M			0.25			0.5		
Conc. PMSE g/L	E_a kJmol^{-1}	$\Delta H^{\#}$ kJmol^{-1}	$-\Delta S^{\#}$ Jmol^{-1}K^{-1}	E_a kJmol^{-1}	$\Delta H^{\#}$ kJmol^{-1}	$-\Delta S^{\#}$ Jmol^{-1}K^{-1}	E_a kJmol^{-1}	$\Delta H^{\#}$ kJmol^{-1}	$-\Delta S^{\#}$ Jmol^{-1}K^{-1}
0	25.63	23.08	140.89	24.73	22.17	143.10	28.52	25.92	130.5
0.03	30.96	28.41	127.65	27.92	25.37	136.28	29.12	26.47	128.8
0.12	40.07	37.52	102.78	31.43	28.87	127.94	32.54	29.89	121.4
0.24	52.38	49.83	70.55	59.16	56.61	45.18	44.89	42.24	25.38

Table 3 Thermodynamic parameter for the PMSE adsorption on MS surface in various concentrations hydrochloric acid at various temperature

HCl (M)	Temp K	K_{ads} M^{-1}	R	ΔG°_{ads} kJmol^{-1}	ΔH°_{ads} kJmol^{-1}	ΔS°_{ads} Jmol^{-1}K^{-1}
0.1	303	1.425	0.999	-11.01	-2.829	-0.027
	313	1.454	0.998	-11.28		
	323	1.317	0.999	-11.55		
0.25	303	1.387	0.999	-10.94	-2.159	-0.029
	313	1.352	0.999	-11.24		
	323	1.315	0.999	-11.52		
0.5	303	1.325	0.972	-10.82		
	313	1.026	0.973	-10.52	-19.45	-0.020
	323	0.822	0.976	-10.25		

Table 4 Surface roughness values of MS surface in the absence and presence of PMSE

Samples	R_a (nm)	R_q (nm)
Specimen immersed in 0.1 M hydrochloric acid	941.8	459.7
Specimen + 0.1 hydrochloric acid + PMSE	30.8	41.9

Table 5 Levels of three operation parameters in Taguchi experiment

Operation Parameter	Level		
	1	2	3
A - HCl concentration (M)	0.1	0.25	0.5
B - Inhibitor concentration (g/L)	0.03	0.12	0.24
C - Temperature (K)	303	313	323

Figures

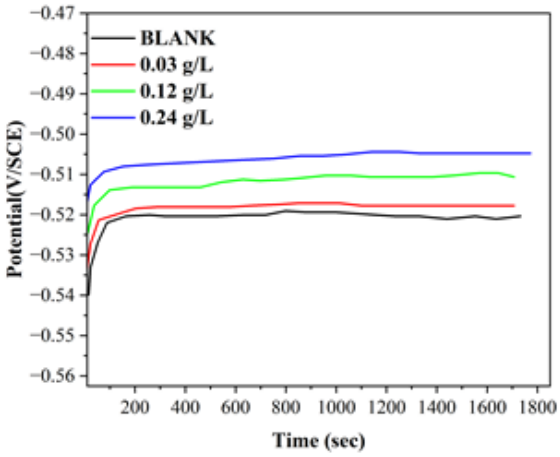

Figure 1

Variation of open circuit potential with time for MS immersed in 0.5 M HCl comprising different amounts of PMSE using saturated calomel electrode (SCE) as the reference electrode.

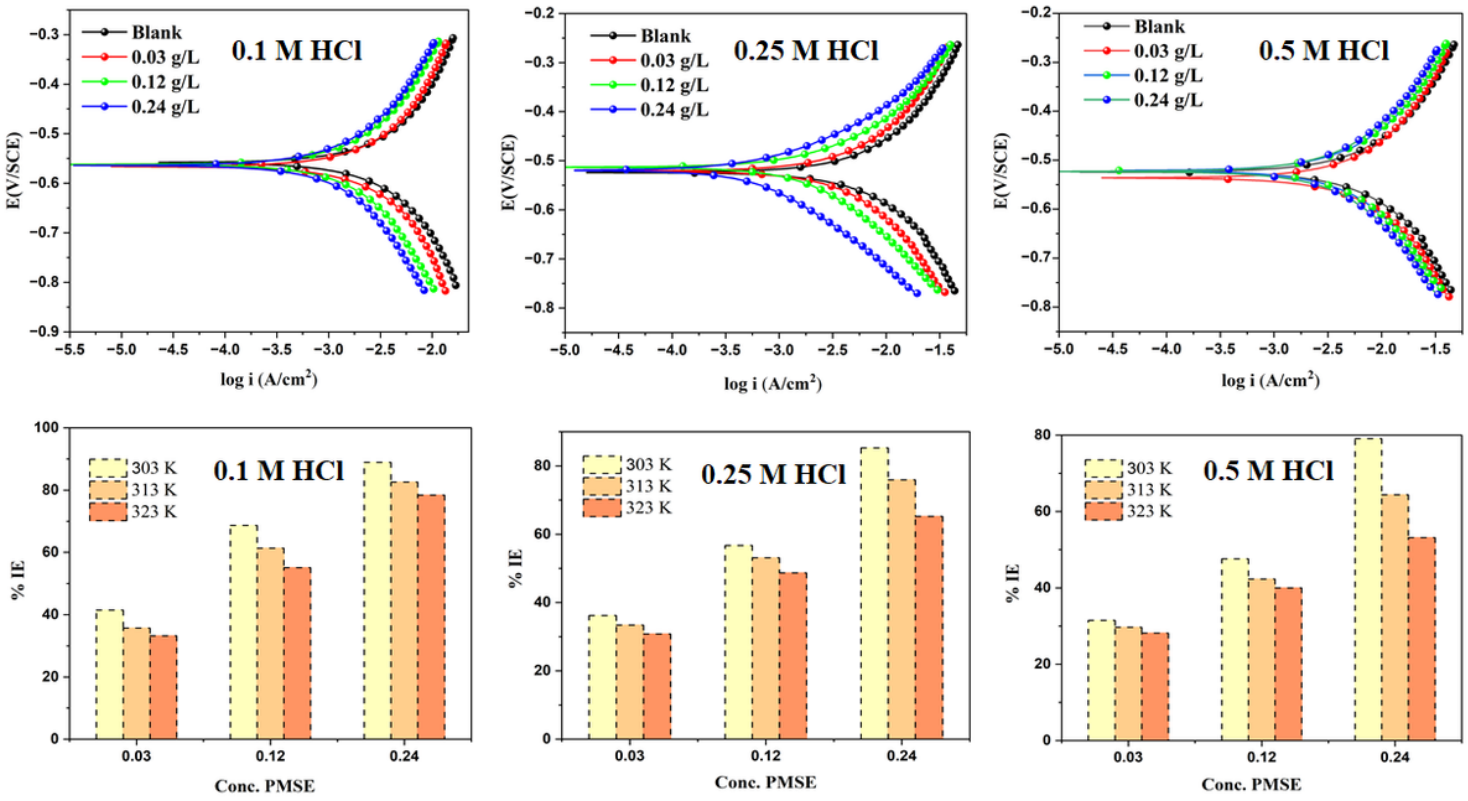

Figure 2

(a) TP curves for the corrosion MS in various concentrations HCl in the absence and presence of different concentrations of PMSE; (b) at different temperatures

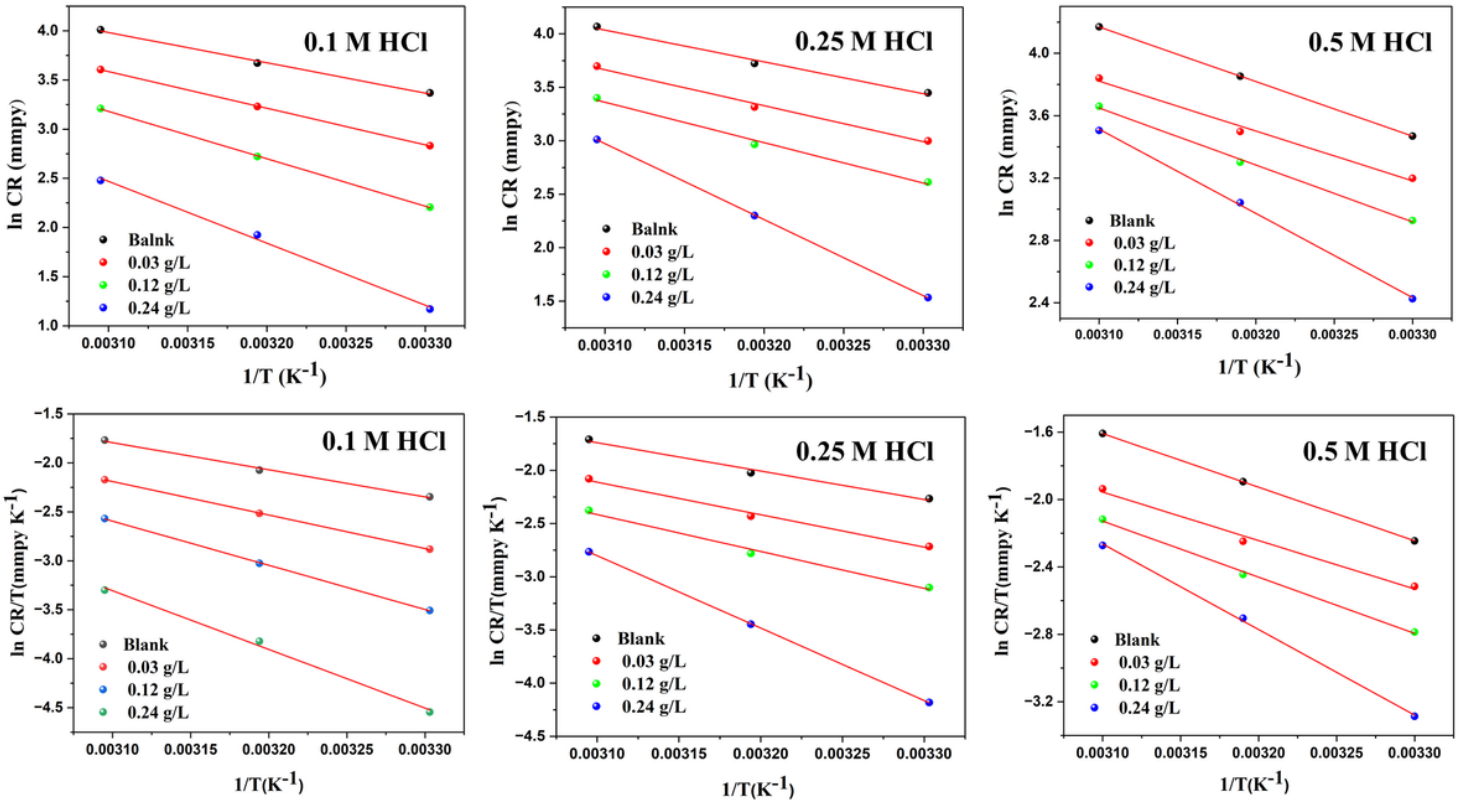

Figure 3

(a) Plot of ln (CR) against 1/T and (b) Plot of ln (CR/T) against 1/T for MS specimen in various concentrations of HCl at different concentrations of PMSE

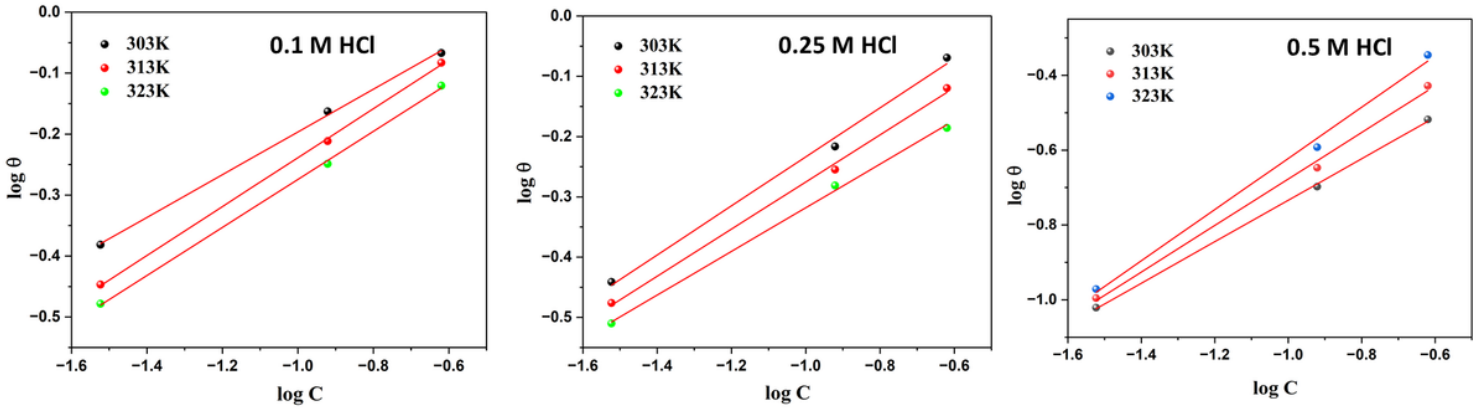

Figure 4

Freundlich's adsorption isotherm for MS in various concentrations of HCl using different concentrations of PMSE

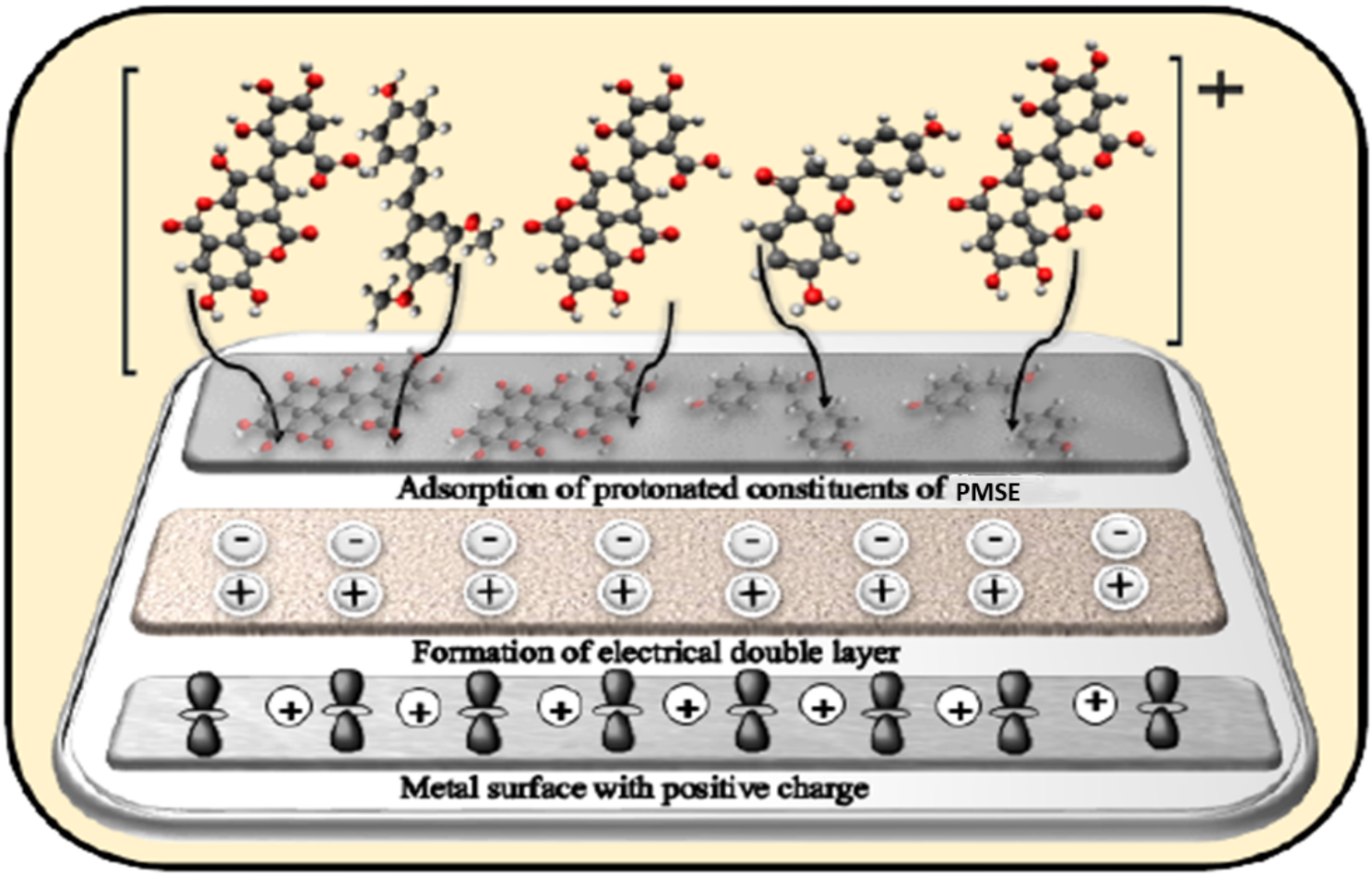

Figure 5

Schematic representation of physical adsorption of the PMSE on the metal surface.

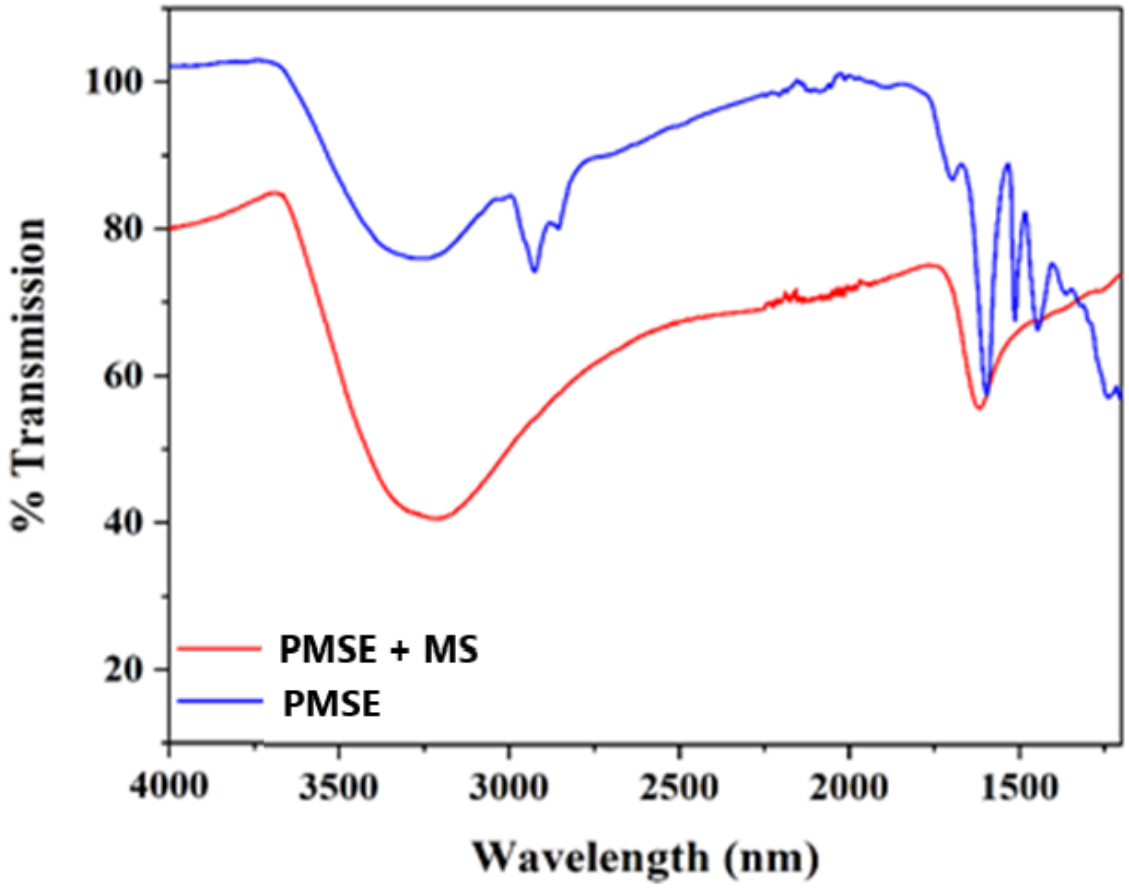

Figure 6

Overlay of the IR spectra of PMSE and product formed after the adsorption of PMSE on MS in 0.1 M HCl

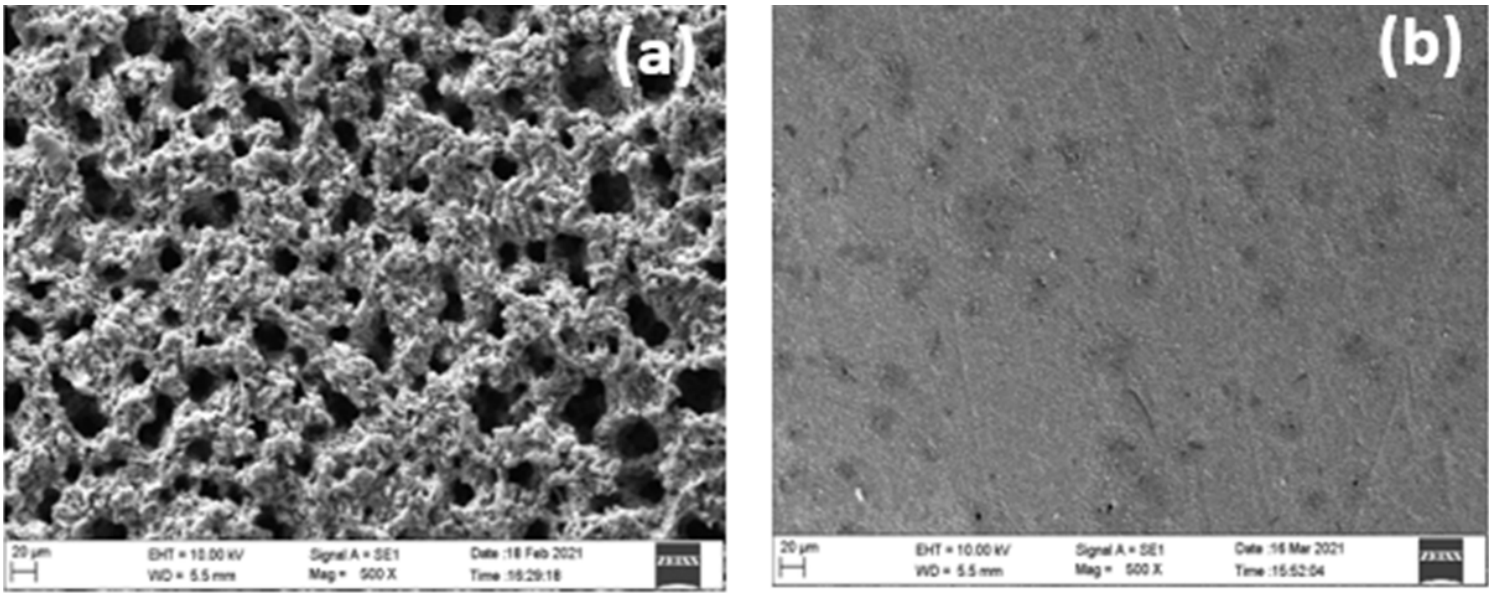

Figure 7

SEM image of MS (a) immersed in 0.5 M HCl (b) 0.5 M HCl + PMSE

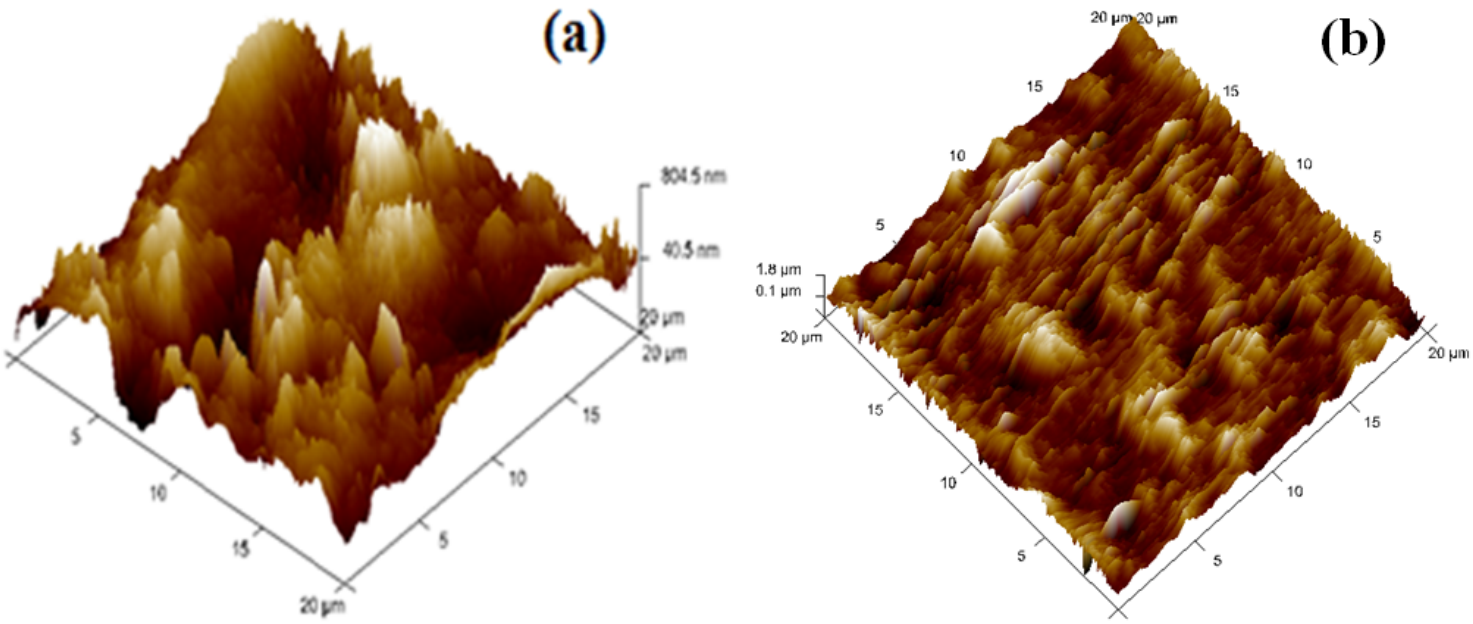

Figure 8

3D image of MS (a) dipped in 0.1 M HCl (b) dipped in 0.1 M HCl + PMSE

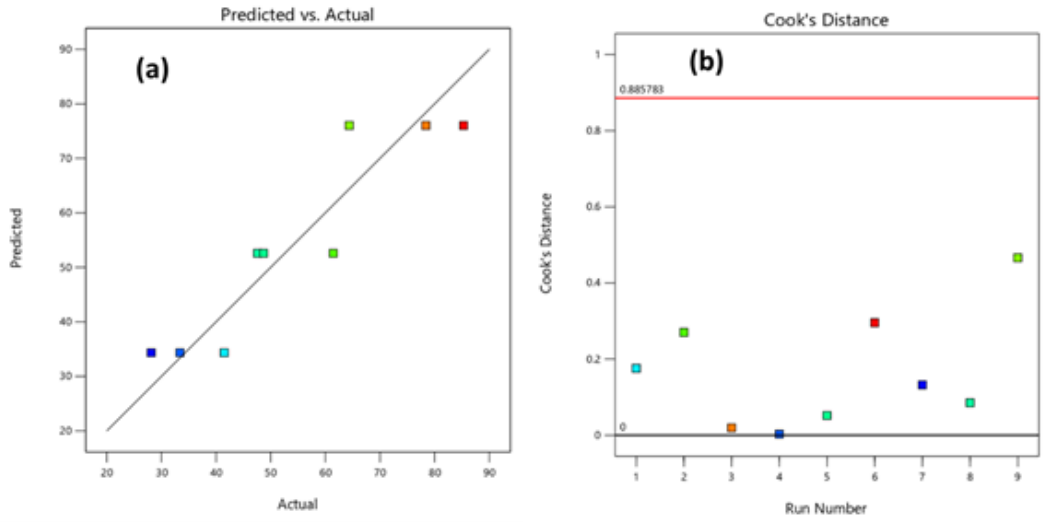

Figure 9

(a) Predicted versus actual values of oil removal percentage; (b) Map of Cook's distance vs run number

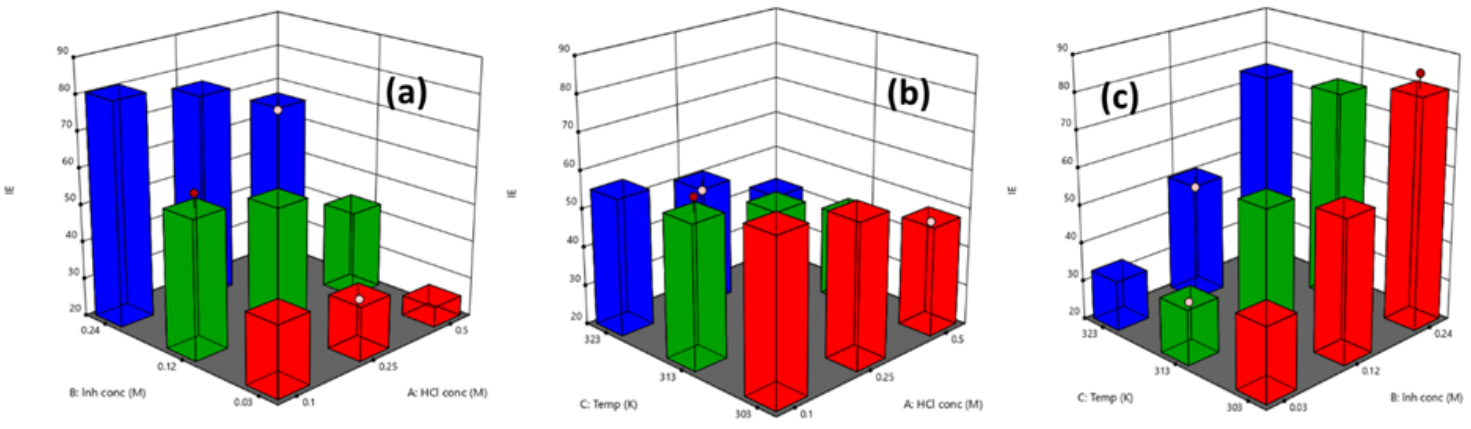

Figure 10

The 3D surface plots of various parameters IE

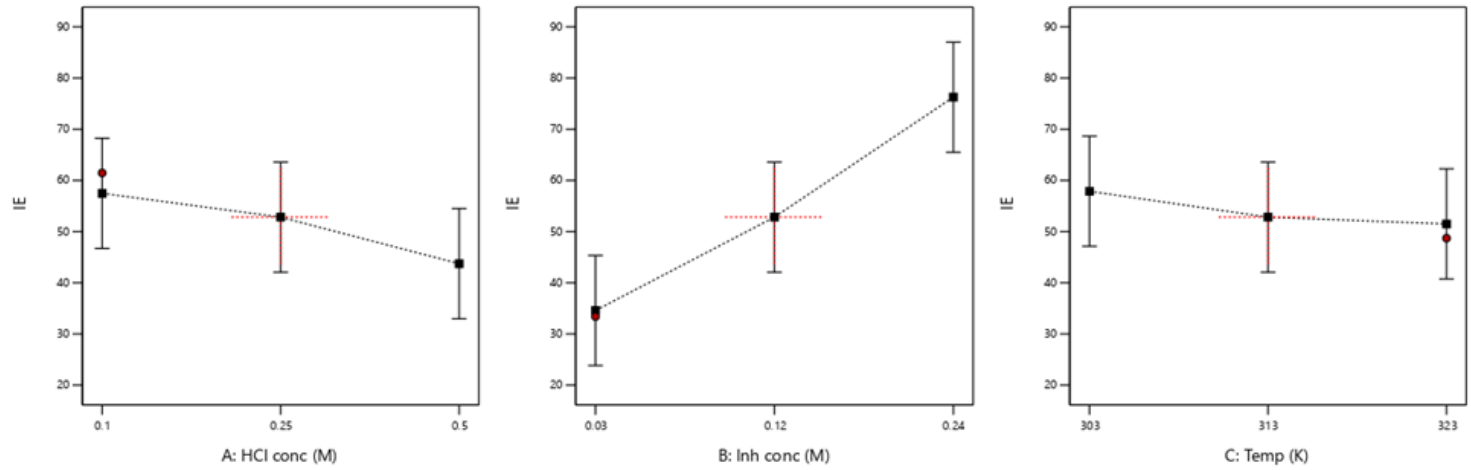

Figure 11

Effect of all parameters on IE, obtained from RSM studies

Supplementary Files

This is a list of supplementary files associated with this preprint. Click to download.

- Graphicalabstarct.tiff